XLI CILAMCE
XLI Ibero-Latin American Congress on Computational Methods in Engineering
16-19 November, 2020 FOZ DO IGUAÇU PARANÁ - BRAZIL

Numerical modeling of venting of particle-driven gravity currents in reservoirs

Malú Grave[1], Jose J. Camata[2], Alvaro L. G. A. Coutinho[1]

[1]*Dept. of Civil Engineering, COPPE/Fedreal University of Rio de Janeiro*
P.O. Box 68506, RJ 21945-970, Rio de Janeiro, Brazil
malugrave@nacad.ufrj.br, alvaro@nacad.ufrj.br
[2]*Dept. of Computer Science,Federal University of Juiz de Fora*
Campus Universidade Federal de Juiz de Fora, Via Local, 4569, 36036-900, MG/Juiz de Fora, Brazil
camata@ice.ufjf.br

Abstract. Sedimentation in reservoirs results in loss of their storage capacity and impacts the fauna where it is located. Therefore, effective sediment management is an important task to increase reservoir lifetime and mitigate the damage that sedimentation may cause. Turbidity currents are the primary source of sediments in reservoirs. Venting them reduces sedimentation. Numerical models are an efficient tool for studying venting. In this work, we have introduced a model to predict the flow of particle-driven gravity currents, and we apply it to study the venting process in reservoirs. The mathematical models result from the incompressible Navier-Stokes equations combined with an advection-diffusion transport equation for suspended sediments. We implement the mathematical model in `libMesh`, an open finite element library that provides a framework for multiphysics numerical simulations. The model is successfully verified and validated using literature data of lock exchange experiments. We test the capability of the model to optimize the venting of turbidity currents as an efficient sediment management strategy for reservoirs. The results show that the concentration field during venting agrees well with observations from laboratory experiments.

Keywords: Gravity currents; Sediment transport; Venting; Computational Fluid Dynamics

1 Introduction

Sedimentation is a problem that most reservoirs face worldwide. Sedimentation causes losses in storage capacity of reservoirs and, consequently, a decrease of energy production [1]; blockage of outlet structures; and downstream impoverishment of river ecosystems, causing coastal land loss and problems with agriculture. Therefore, effective sediment management is an important task to increase reservoir lifetime and mitigate the damage that sedimentation may cause. Turbidity currents are the primary source of sediments in reservoirs. They are a group of density currents formed during yearly floods and transport a large amount of suspended sediment from the watershed into the reservoir. After a certain time, the sediments will settle and, in the long term, fill the reservoir, particularly near the dam and its outlet structures.

Venting represents adequate means to reduce sedimentation in reservoirs where turbidity currents frequently occur. This sediment management strategy aims to route turbid water through bottom outlets as soon as it reaches the dam. Thus, it reduces sedimentation by evacuating the sediments before they settle. One significant advantage is that the reservoir level does not have to be drawn down during these operations, and the outflow discharges remain relatively small. Therefore, venting operations are increasingly appreciated for both economic and environmental reasons [2].

Numerical models are an efficient way to study this relevant process. In this paper, we model gravity currents coupling the Navier-Stokes equations with a sediment transport model, which are solved with the residual-based variational multiscale finite element formulation [3]. We consider adaptive mesh refinement based on the flux jump of the sediment concentration errors in our simulations. All implementations in this work uses the `libMesh` library. `libMesh` is an open-source library that provides a platform for parallel, adaptive, multiphysics finite element simulations [4]. The main advantage of `libMesh` is the possibility of focusing on the implementation of modeling specific features without worrying about adaptivity and code parallelization. Consequently, the effort to

build a high performance computing code tends to be minimized.

This study aims to predict the gravity currents flow within a simple 2D model, and thus, to study the venting efficiency in reservoirs. The remainder of this paper is organized as follows. We start in section 2 with a description of the problem of interest. Then, we present the coupled Navier-Stokes equations for sediment transport. In section 4, we present the sediment transport equations. Section 5 provides the validation of our model and the results obtained. Finally, the paper ends with a summary of our main conclusions.

2 Problem Description

This work studies venting efficiency by changing the flow rate at the outlet in a simple 2D model. The efficiency measure is the global venting efficiency (GVE) index. GVE is defined for a time step t, as the ratio of the total sediment mass entering the reservoir to the vented mass of sediment until t, that is,

$$GVE(t) = \frac{\int_0^t c_{in} Q_{in} d\tau}{\int_0^t c_{out} Q_{out} d\tau}. \tag{1}$$

Therefore, the venting in reservoirs is studied here by reproducing the experimental set-up of Chamoun et al. [2]. It was carried out in a channel with a length $L = 6.7m$, width $b = 0.27m$, and depth $H = 1m$. The channel representing the reservoir is initially filled with clear water, with a water depth of $0.8m$. The channel is constantly fed with $Q_{in} = 0.001m^3/s$ of a sediment-water mixture with a volumetric concentration of 2.3% $(27g/L)$. A bottom outlet $0.12m$ high and $0.09m$ wide is placed at the end of the channel through which water is vented at specifics flow rates. In this work, we simplify the experiment by using a 2D model. Figure 1 shows a schematic of the reproduced model.

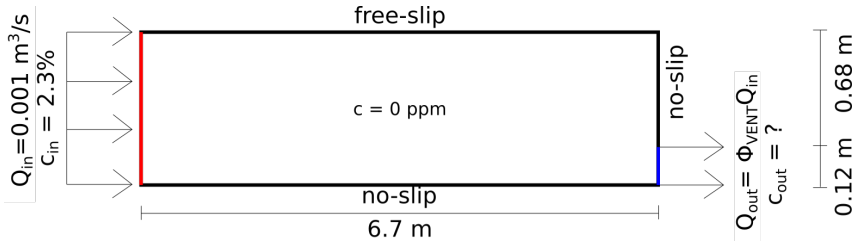

Figure 1. 2D schematic sketch of the experiments.

The inflow velocity is calculated as $u_{in} = Q_{in}/A_{in}$, where A_{in} is the cross-section area of the channel $(0.27m^2)$. Venting degrees, defined as the ratio between outflow and inflow turbidity current discharges, are $\Phi_{VENT} = 30\%, 80\%, 100\%$ and 125%. Thus, we calculate the outflow velocity as $u_{out} = \Phi_{VENT} Q_{in}/A_{out}$, with A_{out} being the cross-section of the venting channel $(0.0108m^2)$. The beginning of venting is synchronized with the arrival of the turbidity current at the outlet. We aim to obtain the sediment concentration that leaves the channel, c_{out}, at this boundary. Sediment properties used in the venting experiments are: particle sizes $d_{10} = 66.5\mu m$, $d_{50} = 140\mu m$ and $d_{90} = 214\mu m$, with a density of $\rho_s = 1160kg/m^3$ and a estimated settling velocity of $u_s = 1.5mm/s$. Here, we consider only the average particle size $d_{50} = 140\mu m$. To model this problem, we couple an advection-diffusion equation for the sediment transport with the Navier-Stokes equations. The following sections briefly present the governing equations.

3 Navier-Stokes Equations

The Navier-Stokes equations govern the fluid flow, which leads to the following nonlinear mathematical problem to be solved: let us consider a space-time domain in which the flow takes place in the domain $\Omega \subset R^{n_{sd}}$, where n_{sd} is the number of space dimensions, along with the interval $[0, t_f]$. Let $\overline{\Gamma}$ denote the boundary of Ω. Find the pressure p and the velocity $\mathbf{u}$ satisfying the following equations,

$$\rho_{mix} \frac{\partial \mathbf{u}}{\partial t} + \rho_{mix} \mathbf{u} \cdot \nabla \mathbf{u} + \nabla p - \nabla \cdot (\mu_{mix} \nabla \mathbf{u}) - \rho_{mix} \mathbf{g} = 0 \text{ in } \Omega \times [0, t_f] \tag{2}$$

$$\nabla \cdot \mathbf{u} = 0 \text{ in } \Omega \times [0, t_f] \tag{3}$$

in which ρ_{mix} is the density of the sediment-water mixture, function of the concentration of sediments in suspension c (usually given in ppm or percentage),

$$\rho_{mix} = c\rho_{sed} + (1-c)\rho_{water}. \tag{4}$$

The Boussinesq approximation states that the density variation is only important in the buoyancy term ($\rho\mathbf{g}$). The advantage of this approximation arises when considering a flow with two densities ρ_1 and ρ_2, where the difference $\rho_1 - \rho_2$ is negligible. Under these circumstances, the only sensible way that acceleration due to gravity $\mathbf{g}$ should enter into the equations of motion is in the reduced gravity $\mathbf{g}'$, where,

$$\mathbf{g}' = \mathbf{g}\frac{\rho_1 - \rho_2}{\rho_2}. \tag{5}$$

Considering $\rho_2 = \rho_{water}$ and $\rho_1 = \rho_{mix}$, we can rewrite equation (2) in function of ρ_{water} as,

$$\rho_{water}\frac{\partial \mathbf{u}}{\partial t} + \rho_{water}\mathbf{u}\cdot\nabla\mathbf{u} + \nabla p - \nabla\cdot(\mu_{water}\nabla\mathbf{u}) - \mathbf{g}c(\rho_{sed} - \rho_{water}) = 0 \tag{6}$$

Equation (6) is supplemented with proper boundary and initial conditions. To approximate the Navier-Stokes equations, we use a finite element Residual-Based Variational Multiscale Formulation (RBVMS). Detailed reviews of the RBVMS formulation can be found in [5–8]. A complete description of the methods used in this work can be seen in [3, 9]

4 Sediment transport equations

The particle transport in suspension can be computed by the concentration distribution by means of an advection-diffusion equation with the form,

$$\frac{\partial c}{\partial t} + (\mathbf{u} + u_s\mathbf{e}^{\mathbf{g}})\cdot\nabla c - \nabla\cdot(\epsilon_s\nabla c) = 0 \text{ in } \Omega\times[0,t_f] \tag{7}$$

in which $\mathbf{e}^{\mathbf{g}}$ is the gravitational acceleration vector, and ϵ_s is the sediment diffusivity. The sediment diffusivity ϵ_s may be correlated with the kinematic viscosity of the fluid by $\epsilon_s = \nu_{water}/Sc$, where Sc is the Schmidt number.

The settling velocity can be estimated by experiments or analytically. Stokes' solution for the drag resistance of the flow past a sphere can be expressed by the simplified Navier-Stokes equation together with the continuity equation in polar coordinates. Using his solution, the following expression for the settling velocity of spherical particles can be derived [10],

$$u_s = \frac{d^2(\rho_{sed} - \rho_{water})g}{18\mu_{water}}. \tag{8}$$

The boundary conditions may be divided into Dirichlet and Neumann BCs.

$$c = c_D \text{ em } \Gamma_D \tag{9}$$

$$((\mathbf{u} + u_s\mathbf{e}^{\mathbf{g}})c - (\epsilon_s\nabla c))\cdot\mathbf{n} = h_T \text{ em } \Gamma_N \tag{10}$$

where c_D is a prescribed concentration and h_T is the total flux of sediments at the boundaries. When no mass exchange happens, as in the free-surface or rigid wall, the total sediment flux is equal to zero. If we have an open channel, the sediments pass through the open boundary. Then, we want to eliminate the terms on the boundary. For that, we define the total flux as, $h_T = ((\mathbf{u} + u_s\mathbf{e}^{\mathbf{g}})c - (\epsilon_s\nabla c))\cdot\mathbf{n}$. Through the sediment surface, i.e., the interface between the sediment and fluid, the sediment exchange depends on the entrainment rate E and the deposition rate D such that $h_T = E - D$. The deposition rate D, in volume per unit horizontal area and time, is determined by $D = u_s c_b$ where c_b is the sediment concentration very near the bed. The entrainment rate could be computed based on empirical models [11, 12]. However, we are not considering entrainment of sediments in this work.

5 Results and Discussion

In this section, we assess the accuracy and performance of the numerical method by solving some problems. First, we validate the code by simulating a lock exchange and comparing it with previous results. Then, we study the venting efficiency.

5.1 Validation of gravity currents

Here, we reproduce the lock exchange experiments of Gladstone et al. [13], also presented in [14]. The lock used in the experiment has dimensions of $20 \times 20 \times 40$ cm. The particles consist of silicon carbide with density $\rho_{sed} = 3217$ kg/m3, and they have diameters $d_{50} = 25 \times 10^{-6}$ m. We consider the settling velocity as $u_s = 0.0005$ m/s. The total particle volume fraction in the lock is 3490 ppm. We employ a reduced value of water viscosity, such as the Reynolds number is $Re = 4000$, to limit the computational cost. We use a 2D model, as presented in Figure 2. For the velocity field, free-slip conditions are imposed at the side and top boundaries, while no-slip is enforced at the bottom wall. Here, we use adaptive mesh refinement. The initial mesh has 356×25 bi-linear quadrilateral elements, and in the subsequent adapted meshes the smallest element has size 0.004 m.

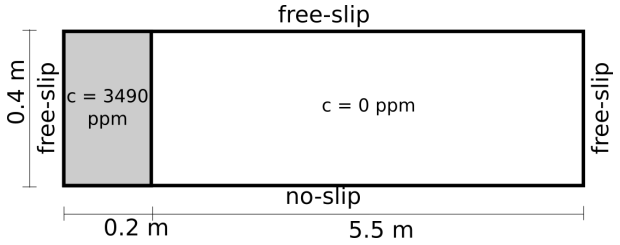

Figure 2. Sketch of the computational setup employed in the present two-dimensional simulation of a particulate lock-exchange current.

All quantities are normalized by the characteristic parameters, that are the characteristic length L_c, characteristic velocity u_b and characteristic concentration C_R, for the sake of results comparison, that is,

$$\mathbf{u}^* = \mathbf{u}/u_b \tag{11}$$

$$\mathbf{x}^* = \mathbf{x}/L_c \tag{12}$$

$$c^* = c/C_R \tag{13}$$

$$t^* = tu_b/L_c \tag{14}$$

For the lock exchange problem, the characteristic length is defined as half the lock height ($L_c = 0.2m$ in this case). Then, the characteristic velocity is given by,

$$u_b = \sqrt{L_c \frac{\rho_{sed} - \rho_{water}}{\rho_{water}} C_R g} \tag{15}$$

Figure 3 compares the final computational deposit profiles against the experimental data of Gladstone et al. [13] and the numerical results of Nasr-Azadani et al. [14]. The curves are normalized such that the results integrate to unity. We observe good agreement between the data.

We also compare the dimensionless friction velocity u_f^*, given by $u_f^* = \sqrt{1/Re \frac{\partial u}{\partial y}}$. The maximum u_f^* observed in the simulation is recorded approximately at time $t^* = 4.2$. Nasr-Azadani et al. [14] have found a maximum value at $t^* = 4.6$ for $R_e = 4000$. Figure 4 displays the spatial distribution of the friction velocity over the bottom wall at $t^* = 4.6$ and Figure 5 the corresponding concentration field. Again, our results are in good agreement with the other data. These results indicate that our code is capable of representing gravity currents.

5.2 Simulation of venting efficiency

Now, we present the results of the venting efficiency based on the experiments of Chamoun et al. [2]. We run four venting degrees and compare our results to those in Chamoun et al. [2] and Wildt et al. [15]. Section 2 describes the setup of this problem. Here, we use adaptive mesh refinement. The initial mesh has 335×40 bi-linear quadrilateral elements, and in the mesh adaptation, we fix the smallest element size to 0.005m. Figure 6 shows the GVE considering each venting degree. The venting time is normalized based on the aspiration height, h_L for the sake of results comparison. According to Jia-Hua [16] the aspiration height is calculated as,

$$h_L = \sqrt[5]{(-1.2)^5 \frac{\rho_{water} Q_{VENT}^2}{(\rho_{sed} - \rho_{water}) g}} \tag{16}$$

The normalized time t^* is given by,

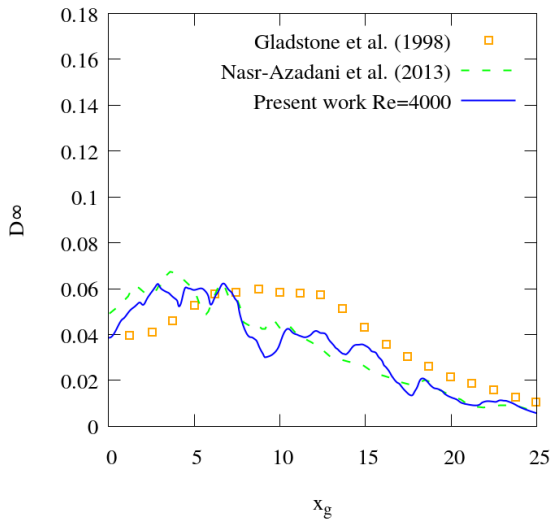

Figure 3. Final deposit profiles for the lock-exchange turbidity current. (x_g is the distance from the lock gate). Solid blue line: present study for $R_e = 4000$. Dashed green line: simulation of Nasr-Azadani et al. [14]. Orange squares: experiments conducted by Gladstone et al. [13].

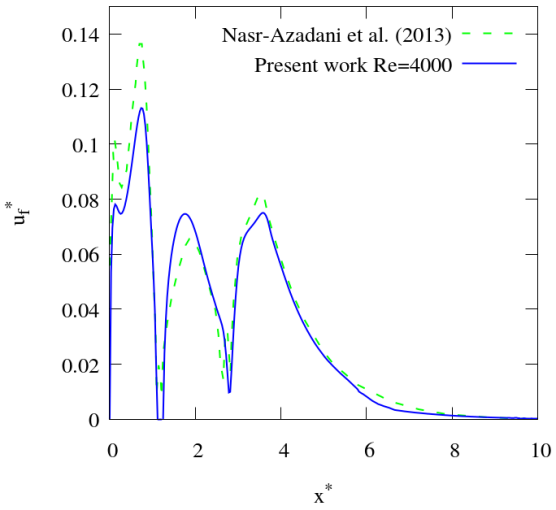

Figure 4. Spatial distribution of friction velocity u_f^* on the bottom wall at time $t^* = 4.6$. Solid blue line: present study. Dashed green line: simulation of Nasr-Azadani et al. [14].

Figure 5. Snapshot of the concentration field (black $c^* = 1$, white $c^* = 0$) at time $t^* = 4.6$.

$$t^* = g' \frac{t - T_{vi}}{h_L} \tag{17}$$

where g' is the absolute reduced gravity and T_{vi} is the time when the venting starts ($T_{vi} = 150s$ in all cases).

The GVE increases rapidly as the venting starts. The slope of the lines is then decreased to a constant value when the flow reaches a steady state. The higher the venting degree, the higher is the global venting efficiency. However, Chamoun et al. [2] have observed that the GVE does not change much with venting degrees higher than 100%. Comparing GVE obtained by our numerical model with GVE of the physical model [2] reveals that venting efficiency is generally overestimated in the simulation. It also happens with the numerical model developed by [15]. A possible explanation for this is the simplifications used. Even though the solver still can capture the phenomenon quite well.

The deposit of sediments for the case with $\Phi = 80\%$ is recorded and compared with [2] and [15]. Figure 7 shows the deposition in different times. In Figure 8, we also show the concentration field for the case with $\Phi = 80\%$ at $t = 150s$, when the venting starts, and $t = 500s$, when the flow already reached the steady-state. At this point, the sediments in suspension leave the channel by the venting process.

6 Conclusions

We coupled the Navier-Stokes equations with a sediment transport model to study the venting efficiency in reservoirs. First, we validated the code by simulating a lock exchange and comparing our results with the literature. We have found good agreement between the data. Then, we studied the venting efficiency with the developed model.

We conclude that a simple 2D model, with several simplifications, may represent the behavior of sediments

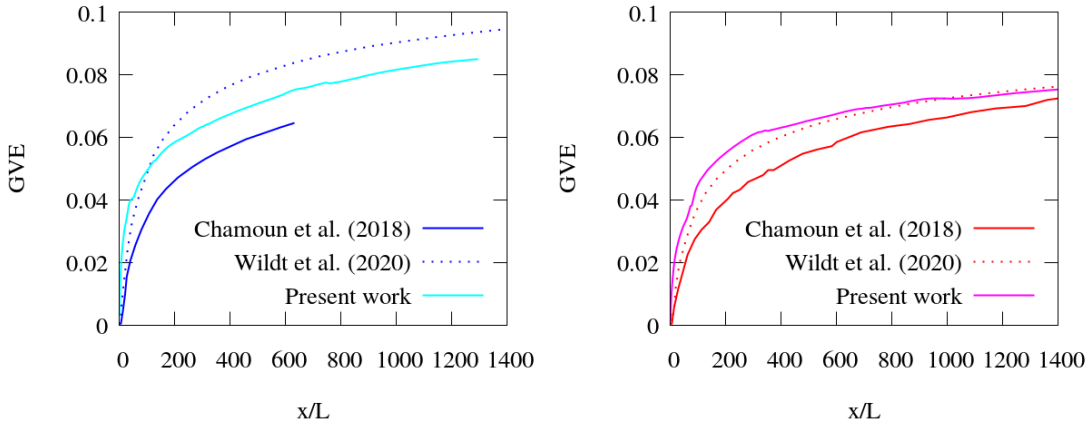

(a) GVE with $\Phi_{VENT} = 125\%$.

(b) GVE with $\Phi_{VENT} = 100\%$.

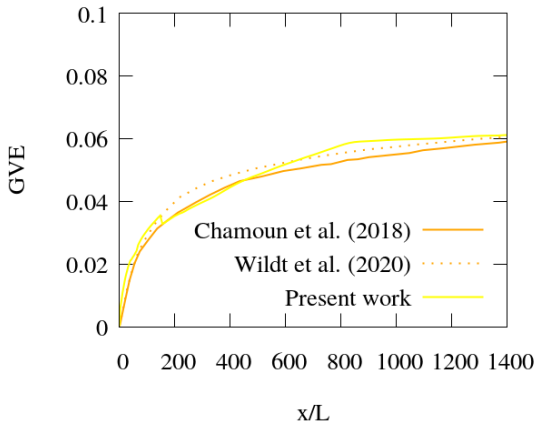

(c) GVE with $\Phi_{VENT} = 80\%$.

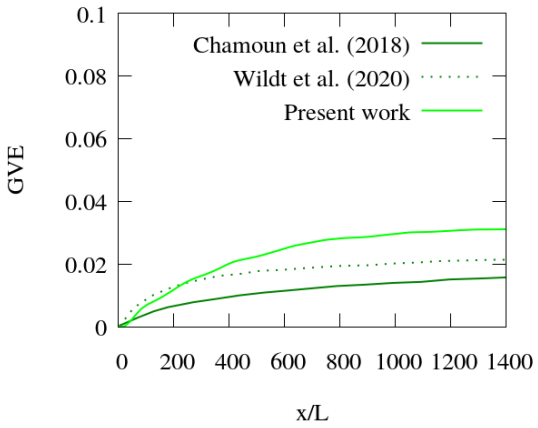

(d) GVE with $\Phi_{VENT} = 30\%$.

Figure 6. Global venting efficiency at different venting degrees Φ_{VENT}. Comparison with the experiments of [2] and the numerical solution of [15].

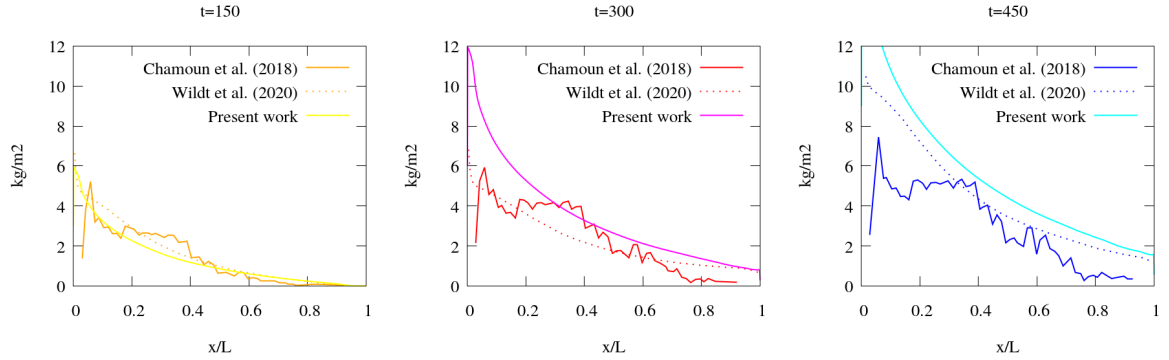

(a) Deposition at t=150 s.

(b) Deposition at t=300 s.

(c) Deposition at t=450 s.

Figure 7. Sediment deposition along the channel at a venting degree of $\Phi = 80\%$. Comparison with the experiments of [2] and the numerical solution of [15].

in a reservoir quite well. Despite the assumed simplifications, the venting efficiency is well predicted, and the deposition is also similar to the experiments. Some improvements that we propose as future work are: to consider multiple granulometries, consider the bed elevation due to the deposition, and simulate 3D cases. It is also interesting to assess other ways to define venting efficiency. One important parameter is how much sediment is deposited at the reservoir bottom and how the venting influences that.

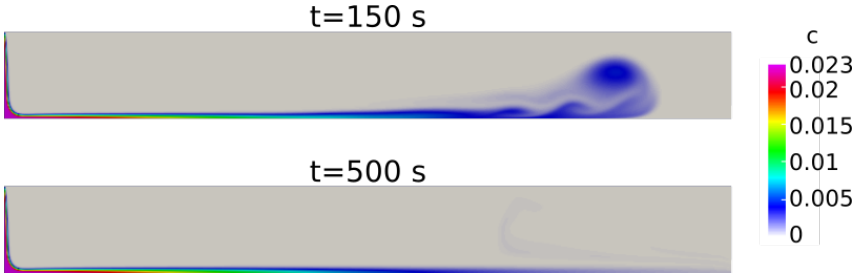

Figure 8. Concentration field at a venting degree of $\Phi = 80\%$ in two different time-steps (top: $t = 150s$, bottom $t = 500s$).

Acknowledgements. This study was financed in part by the Coordenação de Aperfeiçoamento de Pessoal de Nível Superior- Brasil (CAPES) - Finance Code 001. This work is also partially supported by CNPq, FAPERJ, ANP and Petrobras.

Authorship statement. The authors hereby confirm that they are the sole liable persons responsible for the authorship of this work, and that all material that has been herein included as part of the present paper is either the property (and authorship) of the authors, or has the permission of the owners to be included here.

References

[1] de Miranda, R. B. & Mauad, F. F., 2015. Influence of sedimentation on hydroelectric power generation: Case study of a brazilian reservoir. *Journal of Energy Engineering*, vol. 141, n. 3, pp. 04014016.
[2] Chamoun, S., De Cesare, G., & Schleiss, A. J., 2018. Venting of turbidity currents approaching a rectangular opening on a horizontal bed. *Journal of Hydraulic Research*, vol. 56, n. 1, pp. 44–58.
[3] Grave, M., Camata, J. J., & Coutinho, A. L., 2020a. Residual-based variational multiscale 2d simulation of sediment transport with morphological changes. *Computers & Fluids*, vol. 196, pp. 104312.
[4] Kirk, B. S., Peterson, J. W., Stogner, R. H., & Carey, G. F., 2006. libmesh: a c++ library for parallel adaptive mesh refinement/coarsening simulations. *Journal Engineering with Computers*, vol. 22, n. 3, pp. 237–254.
[5] Hughes, T. J. R., Scovazzi, G., & Franca, L. P., 2004. Multiscale and stabilized methods. *Encyclopedia of Computational Mechanics Second Edition*.
[6] Rasthofer, U. & Gravemeier, V., 2017. Recent developments in variational multiscale methods for large-eddy simulation of turbulent flow. *Archives of Computational Methods in Engineering*, pp. 1–44.
[7] Ahmed, N., Rebollo, T. C., John, V., & Rubino, S., 2017. A review of variational multiscale methods for the simulation of turbulent incompressible flows. *Archives of Computational Methods in Engineering*, vol. 24, n. 1, pp. 115–164.
[8] Codina, R., Badia, S., Baiges, J., & Principe, J., 2018. Variational multiscale methods in computational fluid dynamics. *Encyclopedia of Computational Mechanics Second Edition*, pp. 1–28.
[9] Grave, M., Camata, J. J., & Coutinho, A. L. G. A., 2020b. A new convected level-set method for gas bubble dynamics. *Computers & Fluids*, vol. 209, pp. 104667.
[10] Cheng, N.-S., 1997. Simplified settling velocity formula for sediment particle. *Journal of hydraulic engineering*, vol. 123, n. 2, pp. 149–152.
[11] Van Rijn, L. C., 1984. Sediment pick-up functions. *Journal of Hydraulic Engineering*, vol. 110, n. 10, pp. 1494–1502.
[12] Garcia, M. & Parker, G., 1991. Entrainment of bed sediment into suspension. *Journal of Hydraulic Engineering*, vol. 117, n. 4, pp. 414–435.
[13] Gladstone, C., Phillips, J., & Sparks, R., 1998. Experiments on bidisperse, constant-volume gravity currents: propagation and sediment deposition. *Sedimentology*, vol. 45, n. 5, pp. 833–843.
[14] Nasr-Azadani, M., Hall, B., & Meiburg, E., 2013. Polydisperse turbidity currents propagating over complex topography: comparison of experimental and depth-resolved simulation results. *Computers & Geosciences*, vol. 53, pp. 141–153.
[15] Wildt, D., Hauer, C., Habersack, H., & Tritthart, M., 2020. Cfd modelling of particle-driven gravity currents in reservoirs. *Water*, vol. 12, n. 5, pp. 1403.
[16] Jia-Hua, F., 1960. Experimental studies on density currents. *Water and Energy International*, vol. 17, n. 4, pp. 706–729.